Resource Allocation for Visible Light Communication Systems Using Simulated Annealing Based on a Problem-Specific Neighbor Function

UMAIR F. SIDDIQI[1], (Member, IEEE), SADIQ M. SAIT[1,2], (Senior Member, IEEE),
M. SELIM DEMIR[3], (Student Member, IEEE), AND MURAT UYSAL[3], (Fellow, IEEE)

[1]Center for Communications and IT Research, Research Institute, King Fahd University of Petroleum & Minerals, Dhahran 31261, Saudi Arabia
[2]Department of Computer Engineering, King Fahd University of Petroleum & Minerals, Dhahran 31261, Saudi Arabia
[3]Department of Electrical and Electronics Engineering, Özyeğin University, 34794 Istanbul, Turkey

Corresponding author: Sadiq M. Sait (sadiq@kfupm.edu.sa)

ABSTRACT In this paper, we consider a visible light communication (VLC) system with direct current-biased orthogonal frequency division multiplexing (DC-OFDM) and investigate resource allocation for a multi-user environment. Based on the user satisfaction index as a function of data rate, we aim to optimally determine the allocation of the users to different LEDs (acting as access points) and OFDM subcarriers. We propose a simulated annealing-based heuristic to maximize the average user satisfaction index. In an effort to make the proposed solution practically feasible, the runtime of the proposed heuristic is kept less than the channel coherence time, whose value is in order of tens of milliseconds. We evaluate the performance of the proposed heuristic algorithm in different scenarios that vary in the number of users, the number of LEDs, and the separation between users. Our results demonstrate that the proposed heuristic outperforms other well-known heuristics (such as standard simulated annealing, iterative greedy, particle swarm optimization, and tabu search) while achieving good quality solutions within a short execution time, i.e., 40–80 ms.

INDEX TERMS Visible light communications, resource allocation, optimization, simulated annealing, heuristics.

I. INTRODUCTION

Visible light communication (VLC) systems are becoming an effective means of wireless communication [1]. They use light emitting diodes (LEDs) to transmit data, and can be used as a complementary wireless access technology to WiFi and cellular systems. VLC systems feature several advantages such as: (i) a very large bandwidth; (ii) operation in unlicensed spectrum; (iii) useful in places where radio-frequency (RF) signals are not permitted or restricted (for example, some areas in hospitals where the RF signals interfere with patient monitoring systems); and (iv) fading-free channel due to inherent aperture averaging. In addition to the advantages

The associate editor coordinating the review of this manuscript and approving it for publication was Alba Amato.

mentioned above, the ubiquitous availability of LEDs makes possible the widespread adoption of VLC systems in the near future.

The VLC systems employ intensity modulation and direct detection (IM/DD) in which the LEDs modulate the intensity of the light to send data, and the receivers use a photodetector (PD) to retrieve data. Earlier VLC systems employed single-carrier transmission techniques over the frequency-selective channels. However, their data rates remain limited and therefore are not suitable for high-speed applications. The latter VLC systems adopted different types of multi-carrier transmission techniques [2]–[6] and offered high data rates. In particular, orthogonal frequency division multiplexing (OFDM) was employed in the VLC systems with many variations. Among these, DC-biased optical

OFDM (DCO-OFDM) is the most popular due to its simplicity and will be also adopted in this work. In DCO-OFDM, Hermitian symmetry is imposed on the data frame to make the signal real-valued. Then, a DC bias is added to shift the signal into the dynamic range of the LED. DCO-OFDM was already chosen as the mandatory physical layer mode in the upcoming IEEE standard on VLC systems (IEEE 802.15.13) [7].

Orthogonal frequency division multiple access (OFDMA) extends the OFDM to multi-users. In OFDMA, the subcarriers (i.e., frequency slots), time slots, and transmit powers, or any combination of these are treated as resources. Resource allocation is a key technique to optimize the performance of OFDMA. There is already a rich literature on OFDMA-VLC systems. For example, in [8], Wang et al. proposed resource allocation schemes to maximize the so-called β-proportional fairness function. When β is equal to ∞, the function implements a max-min fairness scheduler, and when $\beta = 1$, it reduces to a proportional fairness scheduler. They proposed an iterative algorithm where all users choose a suitable number of resource blocks based on the Lagrangian multiplier method in each iteration of the algorithm. In [9], Bykhovsky and Arnon proposed another resource allocation algorithm that manages subcarrier reuse between different transmitters and power redistribution between different subcarriers under interference constraints. They divided the problem into smaller sub-problems and solved each sub-problem using a simple heuristic. The heuristic of each sub-problem uses the greedy approach to assign the subcarriers to transmitters that offer minimum bit error rate (BER) value. To optimally distribute power among subcarriers, they analyzed three existing heuristics which are based on waterfilling method, convex optimization, and greedy algorithm. In [10], Ling et al. pursued resource allocation problem along with DC-bias optimization. The objective function of DC bias selection comprises terms for both illumination level and clipping noise. For the optimal allocation of power and subcarriers, they proposed three methods based on exhaustive search, dual decomposition, and constant and equal power allocation.

In [11], Seguel et al. investigated the subcarrier allocation to maximize the downlink VLC channel capacity. They modeled the resource allocation problem as a binary and constrained optimization problem and solved it using the Binary Cuckoo Search [12] and Genetic algorithm (GA) [13]. In [14], Feng et al. aimed to maximize the throughput of a multi-user VLC system through user selection, bit loading (i.e., selection of modulation size) and power allocation. They formulated the maximization as a multi-choice knapsack problem and solved it using a heuristic based on dynamic programming. Recently, Demir *et al.* [15], [16] applied the GA and Particle Swarm Optimization (PSO) metaheuristic algorithms for resource allocation in DCO-OFDM systems to maximize the data rate and user fairness index.

The existing applications of metaheuristic algorithms in resource allocation problems of VLC systems discussed above do not account for the channel coherence time.

Soltani *et al.* [17] showed that the coherence time of the indoor VLC channels highly depends on the user location and direction and its value lies within the order of tens of milliseconds. A resource allocation algorithm with a runtime smaller than the channel coherence time can accommodate the dynamic changes in the position of the users without any effect on the data rate for the users. Therefore, keeping the runtime of the algorithm smaller than the channel coherence time is a vital feature for practical implementation of VLC systems.

In this paper, we consider a multi-user DCO-OFDM VLC system. We allocate the subcarriers to users to maximize the average user satisfaction index. This index is defined as the ratio between the actual data rate to the required data rate. It is assumed that although any LED can send data to multiple users, any user can receive data from any one LED without any restriction on the number of subcarriers. For the solution of subcarrier allocation problem under consideration, we need a metaheuristic algorithm with a short runtime.

The metaheuristic algorithms can be divided into two classes based on the number of solutions they store in the memory: (i) population-based, e.g. GA, PSO, etc. ; and (ii) single-solution-based, e.g. simulated annealing (SA), Simulated Evolution (SimE), etc. The population-based metaheuristics usually produce good quality solutions and require a significant amount of runtime. The single-solution-based metaheuristic algorithms are fast and can converge to good solutions within a short time. The resource allocation algorithms in VLC systems demand a runtime in the order of tens of milliseconds; therefore, the single-solution-based metaheuristic algorithms are suitable for this problem.

Taking into account runtime constraints, we apply the SA algorithm to resource allocation problem in VLC systems under consideration, and propose a problem-specific neighbor function. We develop the neighbor function in two steps. In the first step, we represent the solution as a bipartite graph (BG). In the second step, we use the BG representation to develop a robust neighbor function. A BG contains two layers of nodes. The first layer contains LEDs, and the second layer contains the subcarriers. The edges between the LEDs and subcarriers have a label that indicates a user. An edge refers to an allocation in which the user indicated by its label is allocated to the LED and subcarrier denoted by the starting and ending nodes of that edge. One key benefit of representing the solution in the BG is that it becomes easy to distinguish invalid and valid solutions. The simulation results reveal that the proposed problem-specific neighbor function significantly improves the convergence capability of the SA and it can return good solutions using a minimal runtime. A comparison with some standard metaheuristic algorithms such as SA, Tabu search (TS), Iterative Greedy (IG), and PSO indicates that the performance of the proposed heuristic is significantly better than that of the standard ones in most of the usage scenarios under consideration.

This paper is organized as follows. In the second section, we present the system model under consideration. In the
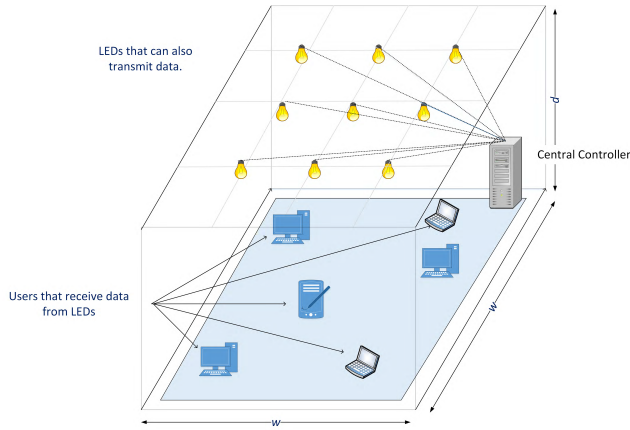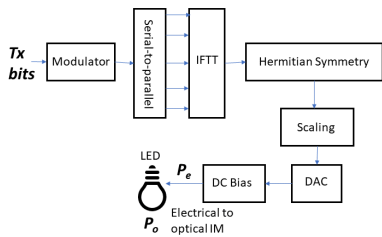
FIGURE 1. Illustration of a VLC system.

FIGURE 2. Simplified block diagram of the DCO-OFDM transmitter.

third section, we first describe the optimization problem, then present the solution representation and optimization heuristic. In the fourth section, we provide simulation results. Finally, we conclude in the last section.

II. SYSTEM MODEL

As illustrated in Fig. 1, we consider the centralized light access network (C-LiAN) architecture proposed in [18]. In C-LiAN, multiple LEDs serve as Access points (AP), and there is a central controller that performs the AP-related computations such as signal processing, interference management, scheduling, and resource allocation. We assume that N users are randomly located in the room, and denoted by $\alpha_U = \{u_0, u_1, ..., u_{N-1}\}$. The ceiling of the room contains uniformly distributed LEDs denoted by $\alpha_L = \{l_0, l_1, ..., l_{L-1}\}$, where L is the number of LEDs. Each LED is assigned up to K subcarriers that can be shared by several users, and subcarriers of LED l_i are denoted as $S_i = \{s_0, s_1, .., s_{K-1}\}$.

The physical layer of the system under consideration builds upon DCO-OFDM. Fig. 2 shows the block diagram of the VLC transmitter. The input bit stream for each LED is mapped into complex symbols according to a modulation scheme, e.g., phase-shift keying (PSK) or quadrature amplitude modulation (QAM). The inverse fast Fourier transform (IFFT) is applied to obtain the time domain signals. The Hermitian symmetry is imposed on the OFDM subcarriers to ensure real-valued signals. This requires that $s_k = s_{K-k}^*$ where $[.]^*$ denotes the complex conjugate operation. It can

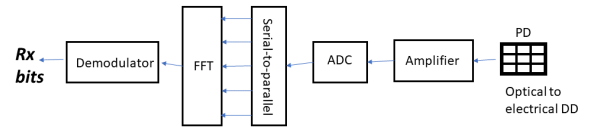**FIGURE 3. Simplified block diagram of the DCO-OFDM receiver.**

be noted that s_0 and $s_{K/2}$ are set equal to zero, and consequently, the number of subcarriers that carry data reduces to $\frac{K}{2} - 1$. The resulting data vector for the LED l_i has the form of $X_i = \begin{bmatrix} 0 \; s_1 \; s_2 \; ... \; s_{K/2-1} \; 0 \; s_{K/2-1}^* \; ... \; s_2^* \; s_1^* \end{bmatrix}$. After K-point IFFT operation, the digital signal is passed through a digital-to-analog converter (DAC). A DC-bias (x_{DC}) is further added and the resulting signal drives the LED. Let P_e denote the electrical power of the input signal. Similarly, let P_o denote the optical power output of the LED. The relationship between the optical and electrical powers can be expressed as $\iota = \frac{P_o}{\sqrt{P_e}}$, where ι is the power ratio. Fig. 3 shows the block diagram of the VLC receiver. After the optical signal is collected by a photodetector (PD), an amplifier is used to mitigate the effects of path loss. After analog-to-digital conversion (ADC), fast Fourier transform (FFT) is performed and the signal is demodulated to recover the data.

In our work, we assume a line-of-sight (LOS) optical channel. The channel coefficient between the LED l_j and user u_i is given by

$$H(l_i, u_j) = \begin{cases} \dfrac{(m+1)A_p \chi^2 T_s(\psi_{l_i,u_j})}{2\pi d_{l_i,u_j}^2 \sin^2(\psi_c)} cos^m(\phi_{l_i,u_j})cos(\psi_{l_i,u_j}) \\ \qquad\qquad\qquad \text{when } \psi_{l_i,\;u_j} \le \psi_c \\ 0 \qquad\qquad\quad \text{when } \psi_{l_i,\;u_j} > \psi_c \end{cases}$$

$$(1)$$

where φ_{l_i,u_j} and ψ_{l_i,u_j} denote, respectively, the angle of irradiance and angle of incidence between the LED l_i and user u_j. As shown in Fig. 4, d_{l_i,u_j} is the distance between the LED l_i and user u_j. ψ_c is the field-of-view (FOV) semi-angle of the user PD. m is the order of Lambertian emission and is equal to $\frac{-1}{\log_2(\cos(\phi_{1/2}))}$ where $\phi_{1/2}$ is the semi-angle of the LED. A_p is the area of the PD, $T_s(\psi_{l_i,u_j})$ is the optical filter gain, B_L denotes the baseband modulation bandwidth, and χ denotes the refractive index.

Assume that user u_j is connected to the LED l_s. The corresponding signal-to-interference-plus-noise ratio (SINR) is given by

$$\gamma_{u_j} = \frac{(\kappa P_o H(l_s, u_j))^2}{(\sum_{l_i \in \aleph}(\kappa P_o H(l_i, u_j))^2 + \iota^2 N_o B_L}$$

$$(2)$$

where $\aleph$ denotes the set of interfering LEDs that interfere with u_j, κ denotes the optical to electrical conversion efficiency of the PDs; N_o denotes the noise power spectral density; and B_L denotes the baseband modulation bandwidth.

In our system, the best modulation order is selected for each subcarrier based on the SINR value. Table 1 shows
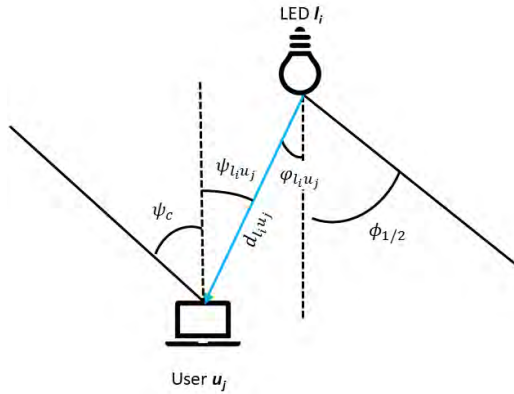
FIGURE 4. LOS channel model.

TABLE 1. Modulation and coding table.

min. SINR (dB)	Modulation	code rate	SE (bit/s/Hz)
-	-	-	0
1	QPSK	0.44	0.8770
3	QPSK	0.59	1.1758
5	16QAM	0.37	1.4766
8	16QAM	0.48	1.9141
9	16QAM	0.60	2.4063
11	64QAM	0.45	2.7305
12	64QAM	0.55	3.3223
14	64QAM	0.65	3.9023
16	64QAM	0.75	4.5234
18	64QAM	0.85	5.1152
20	64QAM	0.93	5.5547

the relationship between the SINR and SE values [8], [19]. We denote the subcarrier s_k of the LED l_i as f_{l_i,s_k}, and its achievable spectral efficiency (SE) as q_{l_i,s_k}. The data rate of the user u_j when it is served by the LED l_i is given by

$$C_j = \frac{2B_L}{M} \sum_{k' \in \Gamma} q_{l_i,s'_k} \quad (3)$$

where Γ denotes the set of subcarriers of LED l_i.

III. RESOURCE ALLOCATION OPTIMIZATION PROBLEM AND SOLUTION

We formulate a subcarrier allocation problem to maximize the user satisfaction in terms of data rate. Users have various type of data traffic and therefore their data rate requirements vary. The degree of satisfaction of any user is the ratio between its actual data rate to the required data rate. Let R_j denote the required data rate for the user u_j. For user u_j, the degree of satisfaction is defined as

$$\theta_j = \begin{cases} \frac{C_j}{R_j} & \text{if } C_j < R_j \\ 1 & \text{otherwise} \end{cases} \quad (4)$$

The objective of our optimization is to maximize the average of the satisfaction indices of all users. Mathematically, we can express the objective function as

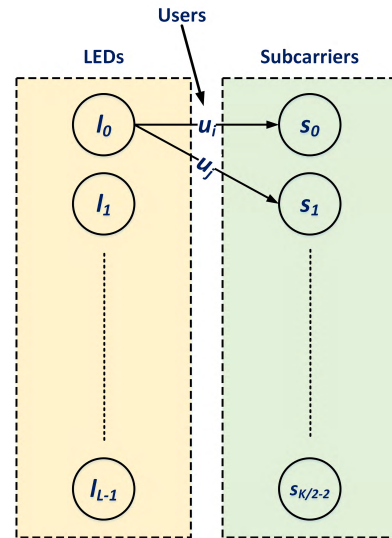$$\text{Maximize } f(\Delta) = \frac{\sum_{j=0...N-1} \theta_j}{N} \quad (5)$$

FIGURE 5. A bipartite graph representation of the solution (Δ).

where Δ represents a possible solution of the resource allocation problem. In the following sub-sections, we discuss the solution representation and optimization heuristic.

A. REPRESENTATION OF THE SOLUTION

The solution representation has a significant influence on the ability of the metaheuristic to search the solution space [20]. In the resource allocation (RA) problem under consideration, an ordinary solution encoding allows both valid and invalid solutions (i.e., a solution that allocate a same user to multiple LEDs). Since we have a strict restriction on the maximum amount to runtime, therefore, we want to use a solution encoding that helps the search to skip invalid solutions.

We propose to use BG [21], [22] to represent the solution (Δ) of the RA problem under consideration. A benefit of BG representation is that it differentiates between valid and invalid solutions, and enable us to improve the runtime of the heuristic by avoiding invalid solutions. Fig. 5 shows the BG representation of the solution. It has two layers of nodes, and the edges connect only the nodes of the first layer with the nodes of the second layer. The nodes of the first layer of the BG represent the LEDs, and the nodes of the second layer represent the subcarriers. The edges between the nodes should have a label equal to any one of the users. We represent the nodes of the first layer as $\{l_0, l_1, ..., l_{L-1}\}$, and nodes of the second layer as $\{s_0, s_1, ..., s_{\frac{K}{2}-2}\}$. We represent an edge using a triplet (l_j, s_k, u_i), where $l_i \in L$ and $s_k \in S$ are the starting and end nodes, and $u_j \in \alpha_U$ is the label. An edge (l_i, s_k, u_j) indicates that the user u_j receives data from the subcarrier s_k of the LED l_i. A random generation of edges may lead to an invalid solution of the RA problem. Therefore, we define some constraints for the BG listed in the following:

1) The out-degree of any node of the first layer should not be more than $\frac{K}{2} - 1$, i.e.:

$$0 \leq deg^+(l_i)) \leq \frac{K}{2} - 1, \quad \forall l_i \in L \quad (6)$$

Algorithm 1 Overview of the SA Algorithm

    Input: $\Delta, T_0, \alpha, \beta, M_0$
    Output: Δ
1   $T = T_0, M = M_0, \Delta_{best} = \Delta$;
2   $c = f(\Delta)$;
3   $c_{best} = c$;
4   **while** *Stopping criterion not reached* **do**
5   Call Metropolis($\Delta, \Delta_{best}, T, M$);
6   Replace M by $\beta \times M$, and T by $\alpha \times T$;
7   **end**
8   return Δ_{best};

---

2) All edges that have the same label should also a common starting node, i.e.:

$$(l_i, s_k, u_j) \in \Delta \rightarrow (l_i', s_k', u_j) \notin \Delta,$$
$$\forall i' \neq j, \ k \text{ and } k' \text{ are mutually unrelated.} \quad (7)$$

3) A node of the first layer should have up to one edge to any node of the second layer, i.e.:

$$(l_i, s_k, u_j) \in \Delta \rightarrow (l_i, s_k, u_j') \notin \Delta, \quad \forall j' \neq i \quad (8)$$

B. OPTIMIZATION HEURISTIC

In this section, we discuss the use of the SA algorithm [13], [23] to solve the RA problem in VLC systems as specified in (5). Algorithm 1 shows the structure of the SA algorithm. The input consists of the solution (Δ) and four parameters (T_0, α, β, and M_0). T_0 is the initial temperature, α represents the cooling rate, β is a constant, and M_0 is the initial value of the number of iterations in the Metropolis function. The value of T_0 should be sufficiently large and the actual value is determined by simulations. We should keep the value of α very close to, but less than, one. The value of β should be one or slightly higher. The Metropolis function consists of two tasks. The first task is to call a neighbor function that creates a new solution from the existing one. The second task is to accept or reject the new solution based on its objective function value and current value of the temperature (T). In the main loop of the SA algorithm, the temperature (T) decreases with iterations and the number of iterations in the Metropolis function (M) could either increase or remain constant. The probability of acceptance of bad moves decreases with decreasing the value of T.

Algorithm 2 outlines the Metropolis function which evolves new solutions in the SA algorithm. The most critical component of the Metropolis function is the call to Neighbor function to generate a new solution from the existing one. If the objective function value of the new solution is better than the existing one, then we always accept the new solution. As the pseudo-code shows, we conditionally accept bad solutions (i.e., solutions which result in a cost lower than the existing one) by using the following steps: (i) Generate a random number between 0 and 1 (*random*) and compare its

---

Algorithm 2 Metropolis Function of the SA Algorithm

    Input: $\Delta, \Delta_{best}, T, M$
    Output: Δ
1   **while** $M > 0$ **do**
2      $\Delta_{new} = \text{Neighbor}(\Delta)$;
3      $T_D = f(\Delta)\text{-}f(\Delta_{new})$;
4   **if** $f(\Delta_{new}) > f(\Delta_{best})$ **then**
5          $\Delta_{best} = \Delta_{new}$
6   **end**
7   **if** $T_D < 0$ *or random* $< e^{-\frac{T_D}{T}}$ **then**
8          $\Delta = \Delta_{new}$
9   **end**
10     $M = M\text{-}1$;
11   **end**
12   return Δ_{best};

Algorithm 3 Neighbor Function of the SA Algorithm

    Input: Δ
    Output: Δ
1   Δ = Make a random change in Δ;
2   **if** Δ *has a constraint violation* **then**
3   Build a set E' that contains all edges of Δ that does not satisfy the constraints specified in (6), (7), and (8) ;
4   Build another set E'' such that $E'' \subseteq E'$, and contains at most one edge for each user, i.e., if $x = (-, -, u_i)$ and $y = (-, -, u_j)$, then $u_i \neq u_j \forall x, y \in E''$. ;
5   Delete edges $\{E' - E''\}$ from Δ
6   **end**
7   return Δ;

---

value with $e^{-\frac{T_D}{T}}$; and (ii) Use the results of the comparison to either accept or reject the new solution.

In the standard SA algorithm, the neighbor function refers to a small random change in the current solution. As mentioned in Section III-A, the current solution Δ is represented by a BG. The neighbor function employed in this work has two steps. The first step is the same as the neighbor function of the standard SA, and we make a random change in the current solution. The new solution created in the first step could be invalid. The second step makes modifications in the solution that are necessary to make it valid again. Through simulations, we found out that when the maximum runtime of the heuristic is restricted by the channel coherence time, traversing the search space through invalid solutions has no advantage in both solution quality and runtime. In this work, we decided to keep the search traverse the positions of only valid solutions. The BG representation enables us to make a solution valid by removing the edges that violate any constraints.

Algorithm 3 gives an overview of the proposed neighbor function. In the first line, we create a random change in Δ,
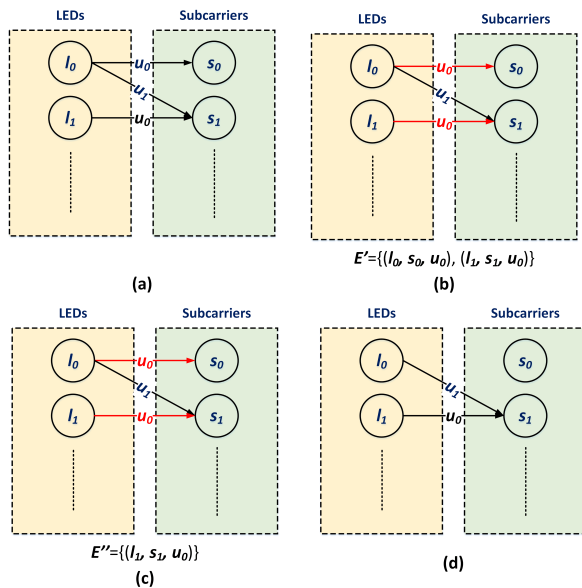
FIGURE 6. Illustration of the removal of the violation of constraint.

a random change refers to one of the following actions: (i) Deletion of an edge which is randomly selected from Δ; and (ii) Adding an edge whose starting node is randomly selected from the set of LEDs $\{l_0, l_1, ..., l_{L-1}\}$, ending node is randomly selected from the set of subcarriers $\{s_0, s_1, ..., s_{\frac{K}{2}-2}\}$, and label is also randomly selected from the set of users $\{u_0, u_1, ..., u_{N-1}\}$. The solution Δ could become invalid after the random change. We can make the solution valid by deleting all edges that violate the constraint. However, deleting all edges that violate any constraint could result in complete vanishing of some users from the solution. Therefore, in this work, we propose a simple method to convert an invalid solution into a valid one while ensuring that each user remains allocated to at least one subcarrier. Algorithm 3 iteratively applies three steps to make the solution valid. The first step is to build a set E' that contains all edges of the graph that violate the constraint. The second step is to build a subset of E' as E'' that contains only one edge for each group of edges from E' that share the same label (or user). The third step is to delete edges from the solution that exists in E' but not in E'', i.e., deletion of the edges that belong to the set $\{E' - E''\}$. The symbol "-" denotes that the value of that element is unrelated to the topic in discussion.

In Fig. 6, we show an example of converting an invalid solution into a valid one by detecting the violations of constraints and deleting the edges to satisfy the constraints. Fig. 6(a) and (b) show a BG that violates the constraint mentioned in (7) because the nodes l_0 and l_1 have edges with label u_0. The set E' contains the two edges that violate the constraint. In Fig. 6(c), we selected one edge for the user u_0. In Fig. 6(d), we deleted an edge which is present in E' but not in E'' to make the solution valid.

Finally, we provide an analysis of the time complexity of the proposed heuristic. We start our analysis with the

time complexity of the Neighbor function. In the proposed heuristic, the solution which is input to the neighbor function is valid. However, it could become invalid inside the Neighbor function after the application of the random change. We observe that a single random change on a valid solution could affect at most one user by assigning subcarriers of different LEDs to it which is a violation of the constraint in (7). The first step in the Neighbor is to make a random change in the solution which has the complexity of $O(1)$. The second step is to make the solution valid and has three sub-steps. The first sub-step can be implemented using two two-level nested loops. The complexity of the first sub-step is equal to $O(K(L + N))$. The second step can also be implemented with a nested loop and has a complexity of $O(LK)$. The third step can be implemented using a loop and has a complexity of $O(K)$. The total complexity of the Neighbor function is equal to $O(K(N + L))$.

The next important analysis is to estimate the number of iterations of the SA algorithm. The general termination criteria of the SA algorithm is the final temperature (T_f). The initial temperature is T_0, and the temperature is reduced by an amount of α in each iteration. The value of temperature in n successive iterations can be expressed with a geometric progression whose first term is T_0 and the nth term is $\alpha^{n-1}T_0$. When n is the last iteration of the SA algorithm, then the final temperature T_f is equal to $\alpha^{n-1}T_0$. The value of n can be determined as $n \geq \frac{ln(T_f) - ln(T_0)}{ln(\alpha)} + 1$. The main loop of the SA algorithm calls the Metropolis function which executes up to M iterations. In the main loop, the value of M increases by a factor of β. The value of M is successive iterations can also be expressed using a geometric progression $\{M, \beta M, .., \beta^{n-1}M\}$. The total number of iterations in both the main loop and the Metropolis function is equal to $\sum_{i=0}^{n-1} \beta^i M$. Using the sum of the geometric progression formula, we can reduce the total number iterations into $M(\frac{\beta^m - 1}{\beta - 1})$. Finally, the complexity of the proposed heuristic becomes equal to $O(M\beta^m K(N + L))$.

IV. SIMULATION RESULTS

In our simulation study, we generated a set of fifty test cases (scenarios) labeled as TS1 to TS50. Table 2 provides the main characteristics of these test cases in terms of the number of users, the number of LEDs, the distance between users, and the dimensions of the rooms, etc. In all test cases, the ceiling contains the LEDs in the form of a grid with a uniform distance (l) between adjacent LEDs. The distribution of users in the room is random with the condition that each user should have an illumination level of at least 400 lx in accordance with European standards lx [24]. As an example, Fig. 7 illustrates the distribution of LEDs and users in test case TS2. We have made the test cases publicly available at [25].

In our simulations, we use the specifications of OSRAM white LEDs (GW KAFHB5.EM) [26] (see Table 3). A suitable selection of DC bias is necessary to keep the LED operate within its dynamic range [27]. For small number of
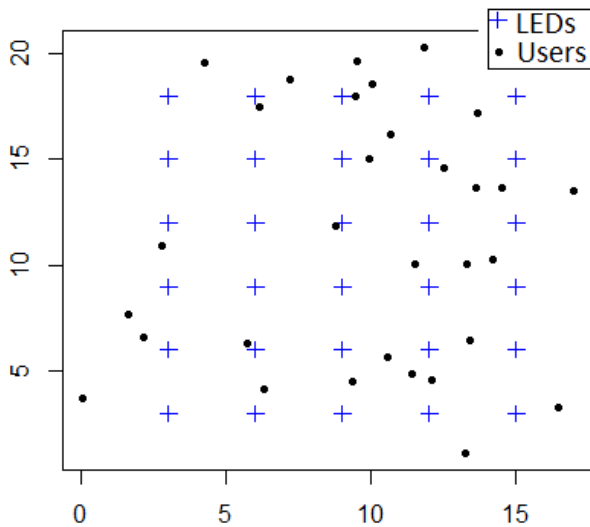
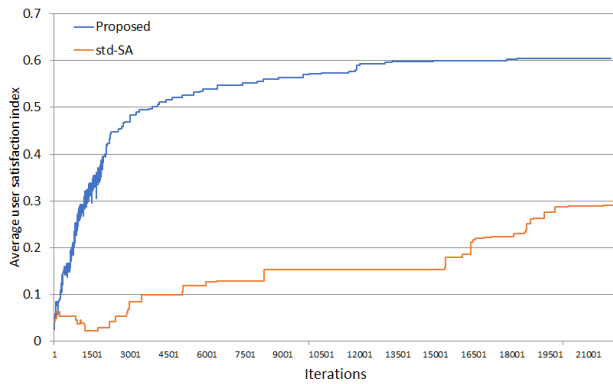**FIGURE 7.** Distributions of the LEDs and users in the test case TS2.

FIGURE 8. Optimization curves of the proposed and std-SA heuristics when the maximum runtime is up to 1s and the parameter have the following values: $\alpha = 0.97$, $\beta = 1$, $T_0 = 100$, $M_0 = 6$.

TABLE 2. Descriptions of test cases.

Problem	Number of users (N)	Number of LEDs (L)	Distance between users u_{avg} (m)	u_{min} (m)	u_{max} (m)	Separation between LEDs l (m)	Dimensions (m^3)
TS1	19	18	8.393	1.249	17.985	3	12×21×2.5
TS2	31	30	9.346	0.778	20.513	3	18×21×2.5
TS3	24	20	8.418	0.77	18.112	3	15×18×2.5
TS4	39	20	8.766	0.886	18.523	3	18×15×2.5
TS5	11	10	6.565	1.103	12.869	3	9×18×2.5
TS6	10	8	4.392	0.755	9.532	3	15×9×2.5
TS7	11	6	3.47	0.858	5.766	2	8×6×2.5
TS8	13	12	5.884	0.74	12.876	2	6×14×2.5
TS9	11	8	3.781	0.854	8.22	3	15×9×2.5
TS10	8	6	3.012	1.048	6.631	3	9×12×2.5
TS11	12	12	7.801	1.248	17.009	3	21×9×2.5
TS12	48	24	6.448	0.523	14.846	2	14×10×2.5
TS13	26	15	5.541	0.631	12.456	2	8×12×2.5
TS14	30	18	7.977	0.781	18.166	3	21×12×2.5
TS15	13	8	4.471	0.827	9.689	3	15×9×2.5
TS16	14	12	6.059	0.778	12.92	2	6×14×2.5
TS17	20	10	4.166	0.558	10.476	2	6×12×2.5
TS18	14	10	3.818	0.92	8.571	2	12×6×2.5
TS19	19	15	5.014	0.931	10.794	2	12×8×2.5
TS20	10	8	4.424	1.455	8.479	2	6×10×2.5
TS21	14	12	6.484	0.714	13.07	2	14×6×2.5
TS22	11	6	3.409	0.813	7.465	2	6×8×2.5
TS23	34	18	5.437	0.529	12.372	2	8×14×2.5
TS24	18	12	6.127	0.782	12.276	3	12×15×2.5
TS25	22	18	6.385	0.596	13.708	2	8×14×2.5
TS26	14	10	4.786	0.752	9.776	2	12×6×2.5
TS27	18	10	4.726	0.596	10.856	2	6×12×2.5
TS28	15	10	5.168	0.558	11.326	2	6×12×2.5
TS29	48	24	9	0.767	20.621	3	21×15×2.5
TS30	22	12	4.907	0.582	13.549	2	14×6×2.5
TS31	60	30	7.129	0.514	16.608	2	12×14×2.5
TS32	14	8	4.757	0.821	10.707	3	9×15×2.5
TS33	15	12	6.025	0.906	11.732	3	12×15×2.5
TS34	12	12	7.714	0.911	16.262	3	9×21×2.5
TS35	15	10	4.709	0.513	9.607	2	12×6×2.5
TS36	12	10	4.811	1.156	10.531	2	6×12×2.5
TS37	7	6	3.755	1.31	6.281	3	12×9×2.5
TS38	36	24	6.097	0.697	14.382	2	10×14×2.5
TS39	24	18	5.948	0.521	14.434	2	14×8×2.5
TS40	10	10	5.128	1.194	10.234	3	9×18×2.5
TS41	14	10	4.846	0.758	11.499	3	18×9×2.5
TS42	36	18	7.33	0.773	17.867	3	21×12×2.5
TS43	38	20	7.817	0.786	17.243	3	18×15×2.5
TS44	41	24	9.399	0.968	21.396	3	21×15×2.5
TS45	25	20	8.176	0.953	16.487	3	15×18×2.5
TS46	22	15	7.073	0.887	15.605	3	18×12×2.5
TS47	37	24	6.708	0.523	16.646	2	10×14×2.5
TS48	11	6	3.456	0.729	6.35	2	6×8×2.5
TS49	25	24	6.528	0.794	13.846	2	14×10×2.5
TS50	20	10	4.931	0.536	11.485	2	12×6×2.5

subcarriers or modulation sizes, peak-to-average power ratio (PAPR) can be kept small [28]. For large values of K, PAPR reduction techniques can be employed [29], [30] or optimal selection of DC bias can be performed [31]. All system parameters used in simulations are listed in Table 3.

We implemented the proposed heuristic in R and C++ using Rcpp, R version 3.1 and GCC version 6.3.0. We used a desktop computer with Intel 2.3 GHz processor and 16 GB of memory. The code does not use multi-threading. The parameters of heuristic algorithm are chosen as $\alpha = 0.95$, $T_0 = 100$, $\beta = 1$, and $M_0 = 6$. We accounted for the stochastic nature of the heuristics by executing up to fifty trials on each test case. As earlier discussed, the coherence time of the line of sight (LOS) channel indoor VLC systems with mobile users is in the order of tens of milliseconds [17]. Therefore we set the maximum runtime of the heuristics to 40 ms, 50 ms, 60 ms, 70 ms, and 80 ms. The proposed heuristic can accommodate mobility of users by determining solutions within the coherence time of the channel.

Initially, we conducted simulations using the test case TS4 to illustrate that the proposed SA heuristic performs better than conventional SA. In the conventional SA (std-SA) [13], the neighbor function is a single random change in the solution. The comparison with SA gives us information about the benefit of using the proposed novel neighbor function over the standard neighbor function. Figs. 8 and 9 show the optimization curves of the conventional and proposed SA heuristics when the runtime is 1s and 80ms, respectively. The curves show that both heuristics benefit from the runtime. However, the use of the new neighbor function enables the proposed heuristic to find much better solutions as compared to the standard SA.

For each test case, we solved the problem up to 50 times, and the following analysis uses the average value of

TABLE 3. System parameters.

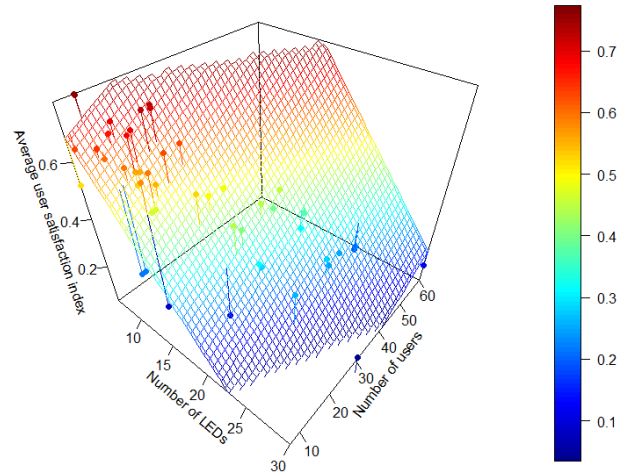| Characteristic	Symbol	Value
Optical power of each LED	P_o	10.4 W [26]
Semiangle at half illumination of the LEDs	$\phi_{1/2}$	60° [26]
Maximum luminous intensity of LEDs	I_o	494 cd [26]
Electrical to optical conversion efficiency	ι	3.2 [26]
FOV of the PDs	ψ_c	85° [16], [24]
Area of the PD	A_p	1 cm² [16], [32]
Optical to electrical conversion efficiency	κ	0.53 A/W [8]
Noise power spectral density	N_0	1×10^{-19} A^2/Hz [16], [32]
Refractive index	χ	1.5 [33], [8]
Gain of optical filter	$T_s(\psi)$	1.0
Number of subcarriers	K	16
Required data rates	R	Poison distribution with mean 10 Mbps

FIGURE 11. Relationship of the solution quality with the number of users and LEDs in the test case when the runtime is 80 ms.
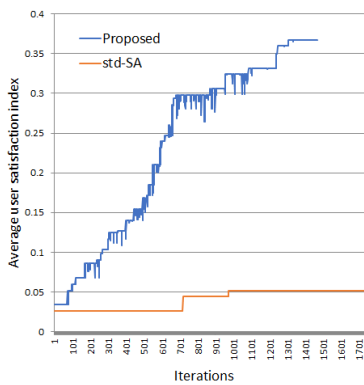

FIGURE 9. Optimization curves of the proposed and std-SA heuristics when the maximum runtime is up to 80ms and the parameter have the following values: $\alpha = 0.95$, $\beta = 1$, $T_0 = 100$, $M_0 = 6$.
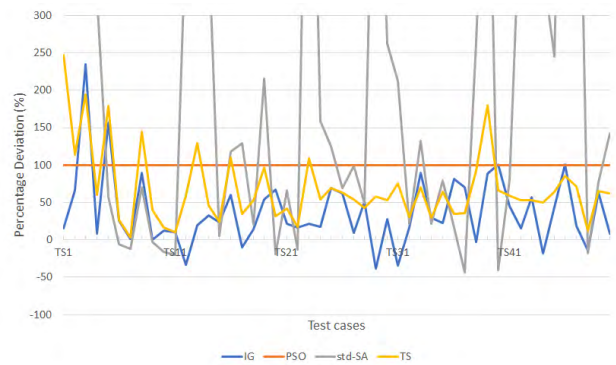

FIGURE 12. The percentage deviation between the mean values of the proposed heuristic with that of the other heuristics when the runtime is 40 ms.

FIGURE 10. The number of test cases that achieve different solution qualities at different runtimes with 95% confidence level.

FIGURE 13. The percentage deviation between the mean values of the proposed heuristic with that of the other heuristics when the runtime is 80 ms.
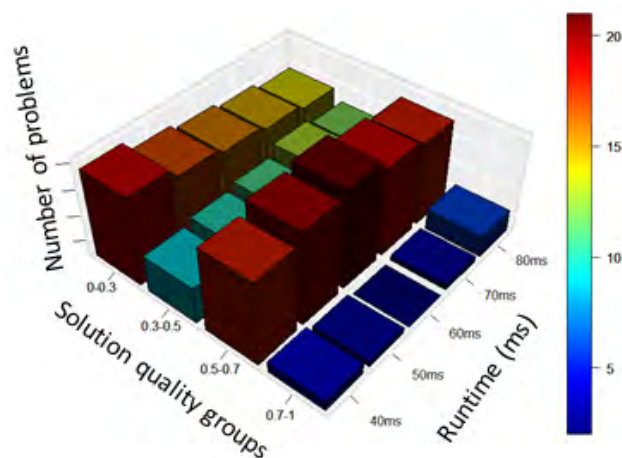
the trials. Complete results of our simulations can be found in the Appendix. In Fig. 10, we classified the test cases into different groups of solution quality using a 95% confidence level. In the classification, we assumed that the lower part of the confidence interval lies within the specified solution quality group. Fig. 10 shows the number of test cases belongs to different groups of the solution quality when the runtime of the heuristic lies from 40 ms to 80 ms. Fig. 10 shows that at any runtime, the group in which the solutions have

TABLE 4. A comparison of the solution quality of the proposed heuristic with existing heuristics using the Wilcoxon rank-sum test.

Runtime (ms)	IG			PSO			std-SA			TS		
	Better	Equal	Inferior	Better	Equal	Inferior	Better	Equal	Inferior	Better	Equal	Inferior
40	39	5	6	47	3	0	39	2	9	47	3	0
50	37	8	5	47	3	0	35	4	11	44	5	1
60	37	6	7	46	4	0	33	5	12	44	4	2
70	37	7	6	46	4	0	31	5	14	42	5	3
80	37	8	5	46	4	0	29	2	19	40	6	4

TABLE 5. Solution quality of the solutions when the heuristics executed for up to 40 ms.

Problem	N	L	u_{min}	Proposed	Std-SA	IG	PSO	TS
TS1	19	18	8.393	0.059 (±0.054)	0.002 (±0.007)	0.051 (±0.022)	-379.881 (±490.3	0.002(±0.007)
TS2	31	30	9.346	0.015 (±0.016)	0.001 (±0.003)	0.009 (±0.012)	-1659.937 (±4211.773	0.001(±0.003)
TS3	24	20	8.418	0.221 (±0.078)	0.016 (±0.02)	0.066 (±0.034)	-879.909 (±1334.62	0.016(±0.02)
TS4	39	20	8.766	0.239 (±0.049)	0.056 (±0.017)	0.22 (±0.037)	-2339.947 (±2882.809	0.056(±0.017)
TS5	11	10	6.565	0.234 (±0.134)	0.149 (±0.141)	0.091 (±0)	-419.759 (±672.759	0.149(±0.141)
TS6	10	8	4.392	0.669 (±0.103)	0.712 (±0.134)	0.532 (±0.059)	-899.675 (±814.394	0.712(±0.134)
TS7	11	6	3.47	0.799 (±0.105)	0.908 (±0.041)	0.788 (±0.104)	-779.658 (±763.705	0.908(±0.041)
TS8	13	12	5.884	0.46 (±0.125)	0.27 (±0.081)	0.243 (±0.033)	-499.783 (±707.099	0.27(±0.081)
TS9	11	8	3.781	0.567 (±0.138)	0.58 (±0.144)	0.568 (±0.122)	-379.733 (±635.313	0.58(±0.144)
TS10	8	6	3.012	0.656 (±0.113)	0.785 (±0.055)	0.583 (±0.055)	-659.621 (±772.205	0.785(±0.055)
TS11	12	12	7.801	0.092 (±0.059)	0.115 (±0.055)	0.083 (±0)	-699.792 (±814.388	0.115(±0.055)
TS12	48	24	6.448	0.118 (±0.036)	0.023 (±0.013)	0.176 (±0.033)	-3859.947 (±6187.582	0.023(±0.013)
TS13	26	15	5.541	0.394 (±0.084)	0.047 (±0.034)	0.329 (±0.065)	-899.907 (±1129.389	0.047(±0.034)
TS14	30	18	7.977	0.319 (±0.058)	0.064 (±0.025)	0.241 (±0.05)	-799.925 (±1399.705	0.064(±0.025)
TS15	13	8	4.471	0.664 (±0.117)	0.628 (±0.146)	0.535 (±0.074)	-739.732 (±803.286	0.628(±0.146)
TS16	14	12	6.059	0.491 (±0.102)	0.225 (±0.09)	0.307 (±0.05)	-879.789 (±772.995	0.225(±0.09)
TS17	20	10	4.166	0.654 (±0.072)	0.286 (±0.101)	0.725 (±0.054)	-699.833 (±886.403	0.286(±0.101)
TS18	14	10	3.818	0.631 (±0.113)	0.525 (±0.103)	0.55 (±0.066)	-359.776 (±631.15	0.525(±0.103)
TS19	19	15	5.014	0.483 (±0.097)	0.153 (±0.042)	0.314 (±0.048)	-759.87 (±822.137	0.153(±0.042)
TS20	10	8	4.424	0.647 (±0.108)	0.803 (±0.124)	0.386 (±0.031)	-739.664 (±803.311	0.803(±0.124)
TS21	14	12	6.484	0.588 (±0.086)	0.353 (±0.06)	0.484 (±0.057)	-399.8 (±699.838	0.353(±0.06)
TS22	11	6	3.409	0.808 (±0.115)	0.931 (±0.045)	0.694 (±0.1)	-539.642 (±676.43	0.931(±0.045)
TS23	34	18	5.437	0.268 (±0.063)	0.029 (±0.019)	0.22 (±0.047)	-939.923 (±1405.678	0.029(±0.019)
TS24	18	12	6.127	0.567 (±0.101)	0.22 (±0.066)	0.481 (±0.07)	-459.847 (±705.935	0.22(±0.066)
TS25	22	18	6.385	0.343 (±0.055)	0.152 (±0.031)	0.203 (±0.031)	-819.89 (±1100.839	0.152(±0.031)
TS26	14	10	4.786	0.525 (±0.124)	0.31 (±0.125)	0.324 (±0.066)	-759.778 (±870.36	0.31(±0.125)
TS27	18	10	4.726	0.689 (±0.084)	0.346 (±0.113)	0.629 (±0.089)	-679.824 (±819.154	0.346(±0.113)
TS28	15	10	5.168	0.661 (±0.087)	0.443 (±0.101)	0.437 (±0.091)	-559.798 (±812.15	0.443(±0.101)
TS29	48	24	9	0.106 (±0.032)	0.013 (±0.014)	0.173 (±0.026)	-4559.956 (±7315.508	0.013(±0.014)
TS30	22	12	4.907	0.544 (±0.066)	0.15 (±0.054)	0.427 (±0.065)	-639.886 (±721.675	0.15(±0.054)
TS31	60	30	7.129	0.07 (±0.02)	0.022 (±0.009)	0.106 (±0.019)	-8019.963 (±12891.208	0.022(±0.009)
TS32	14	8	4.757	0.742 (±0.085)	0.611 (±0.14)	0.638 (±0.084)	-639.755 (±776.16	0.611(±0.14)
TS33	15	12	6.025	0.57 (±0.099)	0.246 (±0.068)	0.3 (±0.044)	-1019.802 (±769.019	0.246(±0.068)
TS34	12	12	7.714	0.542 (±0.072)	0.444 (±0.049)	0.417 (±0)	-879.798 (±772.983	0.444(±0.049)
TS35	15	10	4.709	0.555 (±0.119)	0.308 (±0.126)	0.452 (±0.072)	-319.816 (±652.769	0.308(±0.126)
TS36	12	10	4.811	0.603 (±0.115)	0.518 (±0.113)	0.332 (±0.05)	-719.735 (±756.996	0.518(±0.113)
TS37	7	6	3.755	0.516 (±0.135)	0.916 (±0.091)	0.303 (±0.069)	-659.545 (±626.297	0.916(±0.091)
TS38	36	24	6.097	0.183 (±0.039)	0.05 (±0.019)	0.188 (±0.027)	-2459.935 (±3845.008	0.05(±0.019)
TS39	24	18	5.948	0.317 (±0.08)	0.042 (±0.037)	0.168 (±0.038)	-1019.908 (±936.568	0.042(±0.037)
TS40	10	10	5.128	0.205 (±0.186)	0.343 (±0.125)	0.102 (±0.007)	-419.732 (±672.761	0.343(±0.125)
TS41	14	10	4.846	0.551 (±0.101)	0.305 (±0.116)	0.379 (±0.06)	-459.77 (±676.406	0.305(±0.116)
TS42	36	18	7.33	0.304 (±0.065)	0.053 (±0.018)	0.263 (±0.037)	-1999.932 (±4430.866	0.053(±0.018)
TS43	38	20	7.817	0.201 (±0.053)	0.039 (±0.015)	0.128 (±0.029)	-1939.944 (±3253.941	0.039(±0.015)
TS44	41	24	9.399	0.132 (±0.042)	0.029 (±0.015)	0.162 (±0.023)	-3699.951 (±6434.119	0.029(±0.015)
TS45	25	20	8.176	0.174 (±0.053)	0.05 (±0.018)	0.121 (±0.035)	-1139.911 (±1309.462	0.05(±0.018)
TS46	22	15	7.073	0.424 (±0.089)	0.043 (±0.037)	0.211 (±0.054)	-539.892 (±734.285	0.043(±0.037)
TS47	37	24	6.708	0.12 (±0.043)	0.014 (±0.014)	0.101 (±0.023)	-3519.936 (±5127.918	0.014(±0.014)
TS48	11	6	3.456	0.737 (±0.107)	0.904 (±0.055)	0.859 (±0.078)	-879.703 (±689.242	0.904(±0.055)
TS49	25	24	6.528	0.198 (±0.052)	0.111 (±0.018)	0.121 (±0.006)	-1119.925 (±1836.595	0.111(±0.018)
TS50	20	10	4.931	0.611 (±0.083)	0.252 (±0.096)	0.566 (±0.055)	-639.844 (±802.037	0.252(±0.096)

quality between 0.5-0.7 have the maximum number of test cases. The histogram also indicates that the size of the group 0-0.3 decreases with the increase in the runtime. It means that with the increase in runtime, the solution quality also improves.

Fig. 11 shows with the help of a regression plane the relationship of the solution quality on the number of users (N) and the number of LEDs (L) present in the room. From the figure it can be seen that the problems that have a smaller number of users and LEDs converge to good quality solutions

TABLE 6. Solution quality of the solutions when the heuristics executed for up to 50 ms.

Problem	N	L	u_{min}	Proposed	Std-SA	IG	PSO	TS
TS1	19	18	8.393	0.061 (±0.059)	0.008 (±0.015)	0.055 (±0.021)	-299.887 (±580.268	0.008(±0.015)
TS2	31	30	9.346	0.02 (±0.019)	0.003 (±0.007)	0.007 (±0.013)	-979.941 (±2094.599	0.003(±0.007)
TS3	24	20	8.418	0.282 (±0.074)	0.018 (±0.021)	0.077 (±0.038)	-1159.905 (±1543.371	0.018(±0.021)
TS4	39	20	8.766	0.279 (±0.057)	0.06 (±0.024)	0.241 (±0.037)	-1479.947 (±2612.684	0.06(±0.024)
TS5	11	10	6.565	0.218 (±0.107)	0.239 (±0.142)	0.093 (±0.013)	-599.731 (±755.885	0.239(±0.142)
TS6	10	8	4.392	0.663 (±0.112)	0.811 (±0.111)	0.549 (±0.068)	-839.689 (±765.559	0.811(±0.111)
TS7	11	6	3.47	0.796 (±0.091)	0.92 (±0.041)	0.789 (±0.107)	-819.658 (±690.743	0.92(±0.041)
TS8	13	12	5.884	0.443 (±0.148)	0.348 (±0.101)	0.253 (±0.03)	-659.793 (±772.211	0.348(±0.101)
TS9	11	8	3.781	0.588 (±0.149)	0.675 (±0.092)	0.57 (±0.113)	-359.729 (±631.139	0.675(±0.092)
TS10	8	6	3.012	0.646 (±0.098)	0.808 (±0.054)	0.597 (±0.052)	-619.629 (±567.48	0.808(±0.054)
TS11	12	12	7.801	0.09 (±0.047)	0.147 (±0.101)	0.083 (±0)	-599.798 (±728.401	0.147(±0.101)
TS12	48	24	6.448	0.147 (±0.047)	0.029 (±0.014)	0.201 (±0.031)	-2579.95 (±5678.787	0.029(±0.014)
TS13	26	15	5.541	0.426 (±0.085)	0.065 (±0.03)	0.385 (±0.067)	-839.904 (±1094.704	0.065(±0.03)
TS14	30	18	7.977	0.365 (±0.055)	0.071 (±0.033)	0.268 (±0.066)	-699.927 (±1147.316	0.071(±0.033)
TS15	13	8	4.471	0.686 (±0.116)	0.775 (±0.114)	0.527 (±0.085)	-639.734 (±721.645	0.775(±0.114)
TS16	14	12	6.059	0.515 (±0.11)	0.302 (±0.109)	0.332 (±0.058)	-579.803 (±702.467	0.302(±0.109)
TS17	20	10	4.166	0.682 (±0.072)	0.361 (±0.1)	0.734 (±0.048)	-339.83 (±626.306	0.361(±0.1)
TS18	14	10	3.818	0.629 (±0.135)	0.605 (±0.1)	0.547 (±0.082)	-319.787 (±586.929	0.605(±0.1)
TS19	19	15	5.014	0.466 (±0.073)	0.168 (±0.05)	0.303 (±0.046)	-959.861 (±902.598	0.168(±0.05)
TS20	10	8	4.424	0.619 (±0.122)	0.873 (±0.078)	0.401 (±0.038)	-459.629 (±676.432	0.873(±0.078)
TS21	14	12	6.484	0.589 (±0.076)	0.393 (±0.074)	0.487 (±0.053)	-499.793 (±814.395	0.393(±0.074)
TS22	11	6	3.409	0.784 (±0.115)	0.941 (±0.041)	0.739 (±0.128)	-459.646 (±676.427	0.941(±0.041)
TS23	34	18	5.437	0.308 (±0.073)	0.028 (±0.027)	0.239 (±0.056)	-779.919 (±1200.177	0.028(±0.027)
TS24	18	12	6.127	0.596 (±0.097)	0.244 (±0.075)	0.526 (±0.071)	-499.851 (±788.935	0.244(±0.075)
TS25	22	18	6.385	0.392 (±0.083)	0.161 (±0.026)	0.226 (±0.043)	-579.886 (±758.357	0.161(±0.026)
TS26	14	10	4.786	0.544 (±0.133)	0.427 (±0.15)	0.319 (±0.042)	-419.772 (±702.456	0.427(±0.15)
TS27	18	10	4.726	0.727 (±0.096)	0.421 (±0.129)	0.658 (±0.081)	-759.827 (±822.138	0.421(±0.129)
TS28	15	10	5.168	0.673 (±0.1)	0.55 (±0.116)	0.451 (±0.083)	-499.804 (±677.635	0.55(±0.116)
TS29	48	24	9	0.142 (±0.043)	0.015 (±0.017)	0.191 (±0.033)	-3179.952 (±7032.543	0.015(±0.017)
TS30	22	12	4.907	0.574 (±0.075)	0.192 (±0.066)	0.457 (±0.079)	-419.89 (±574.633	0.192(±0.066)
TS31	60	30	7.129	0.076 (±0.022)	0.023 (±0.01)	0.109 (±0.023)	-3959.964 (±8121.426	0.023(±0.01)
TS32	14	8	4.757	0.711 (±0.115)	0.714 (±0.127)	0.691 (±0.092)	-679.745 (±767.688	0.714(±0.127)
TS33	15	12	6.025	0.586 (±0.083)	0.307 (±0.095)	0.308 (±0.051)	-619.809 (±696.615	0.307(±0.095)
TS34	12	12	7.714	0.559 (±0.087)	0.442 (±0.052)	0.417 (±0)	-599.807 (±728.399	0.442(±0.052)
TS35	15	10	4.709	0.573 (±0.12)	0.458 (±0.146)	0.488 (±0.076)	-539.815 (±761.564	0.458(±0.146)
TS36	12	10	4.811	0.623 (±0.11)	0.678 (±0.145)	0.348 (±0.063)	-559.716 (±704.498	0.678(±0.145)
TS37	7	6	3.755	0.473 (±0.126)	0.944 (±0.048)	0.303 (±0.045)	-759.536 (±715.978	0.944(±0.048)
TS38	36	24	6.097	0.213 (±0.046)	0.057 (±0.015)	0.197 (±0.026)	-2559.941 (±3296.014	0.057(±0.015)
TS39	24	18	5.948	0.364 (±0.083)	0.043 (±0.031)	0.194 (±0.046)	-619.896 (±830.303	0.043(±0.031)
TS40	10	10	5.128	0.184 (±0.133)	0.52 (±0.196)	0.102 (±0.008)	-319.696 (±620.697	0.52(±0.196)
TS41	14	10	4.846	0.534 (±0.095)	0.449 (±0.128)	0.393 (±0.068)	-559.764 (±732.874	0.449(±0.128)
TS42	36	18	7.33	0.368 (±0.063)	0.06 (±0.024)	0.299 (±0.053)	-879.929 (±1858.673	0.06(±0.024)
TS43	38	20	7.817	0.236 (±0.057)	0.043 (±0.015)	0.157 (±0.042)	-819.947 (±1240.308	0.043(±0.015)
TS44	41	24	9.399	0.165 (±0.053)	0.028 (±0.017)	0.161 (±0.028)	-3599.949 (±5921.244	0.028(±0.017)
TS45	25	20	8.176	0.205 (±0.072)	0.057 (±0.028)	0.153 (±0.046)	-1059.91 (±2113.207	0.057(±0.028)
TS46	22	15	7.073	0.452 (±0.087)	0.061 (±0.049)	0.259 (±0.052)	-639.883 (±692.803	0.061(±0.049)
TS47	37	24	6.708	0.144 (±0.044)	0.012 (±0.013)	0.116 (±0.028)	-1419.939 (±2186.135	0.012(±0.013)
TS48	11	6	3.456	0.721 (±0.112)	0.926 (±0.047)	0.883 (±0.051)	-819.683 (±719.682	0.926(±0.047)
TS49	25	24	6.528	0.218 (±0.048)	0.119 (±0.017)	0.123 (±0.006)	-659.916 (±1099.355	0.119(±0.017)
TS50	20	10	4.931	0.656 (±0.071)	0.333 (±0.112)	0.623 (±0.065)	-259.841 (±527.219	0.333(±0.112)

given a limitation on the maximum runtime (80 ms). From the figure we can also determine the actual values of the number of users and LEDs present in the test cases that converged to different solution qualities such as the following: The test cases that converged to solution quality better than 0.7 have the number of users between 11-20, and the number of LEDs between 6-10. The test cases that have solution quality between 0.5 to 0.7 have the number of users and LEDs lie in the range from 7-22 and 6-15, respectively. The group of test cases that have solution quality between 0.3 to 0.5 has the number of users and number of LEDs between 13-29 and 12-20, respectively.

We further compared our heuristic with four other heuristics. The first is the std-SA [13]. The second is the

IG heuristic [13], which is a competitor for SA because of its quick convergence and simple design that closely matches with that of the SA. The third is PSO for the RA problem as proposed by Demir *et al.* [16]. The fourth is the standard TS algorithm [13]. We implemented the std-SA and IG using the C++ programming language and executed them on the same platform as the proposed heuristic. The IG heuristic consists of the following steps: (i) a random initialization of the solution; and (ii) an optimization loop that is sub-divided into the following: (a) the destruction of the current solution and (b) the greedy construction of the current solution. The destruction step deletes up to 10% of the elements of the current solution. The greedy construction step finds the best value for each element that was deleted in the destruction

TABLE 7. Solution quality of the solutions when the heuristics executed for up to 60 ms.

Problem	N	L	u_{min}	Proposed	Std-SA	IG	PSO	TS
TS1	19	18	8.393	0.089 (±0.076)	0.008 (±0.017)	0.059 (±0.024)	-279.89 (±496.502	0.008(±0.017)
TS2	31	30	9.346	0.032 (±0.031)	0.001 (±0.005)	0.009 (±0.013)	-959.934 (±3410.415	0.001(±0.005)
TS3	24	20	8.418	0.307 (±0.074)	0.027 (±0.024)	0.112 (±0.026)	-499.909 (±707.096	0.027(±0.024)
TS4	39	20	8.766	0.31 (±0.055)	0.064 (±0.022)	0.239 (±0.046)	-1299.95 (±2101.991	0.064(±0.022)
TS5	11	10	6.565	0.218 (±0.13)	0.231 (±0.131)	0.091 (±0)	-579.72 (±810.346	0.231(±0.131)
TS6	10	8	4.392	0.658 (±0.093)	0.823 (±0.112)	0.529 (±0.075)	-919.695 (±751.578	0.823(±0.112)
TS7	11	6	3.47	0.775 (±0.098)	0.908 (±0.045)	0.809 (±0.102)	-579.661 (±609.127	0.908(±0.045)
TS8	13	12	5.884	0.449 (±0.12)	0.366 (±0.11)	0.261 (±0.038)	-579.787 (±784.79	0.366(±0.11)
TS9	11	8	3.781	0.596 (±0.144)	0.71 (±0.115)	0.634 (±0.137)	-539.702 (±645.513	0.71(±0.115)
TS10	8	6	3.012	0.681 (±0.114)	0.81 (±0.063)	0.601 (±0.049)	-559.622 (±674.889	0.81(±0.063)
TS11	12	12	7.801	0.085 (±0.012)	0.161 (±0.095)	0.083 (±0)	-499.793 (±677.606	0.161(±0.095)
TS12	48	24	6.448	0.17 (±0.038)	0.026 (±0.015)	0.223 (±0.037)	-2999.942 (±6565.216	0.026(±0.015)
TS13	26	15	5.541	0.448 (±0.095)	0.07 (±0.043)	0.422 (±0.072)	-799.9 (±699.855	0.07(±0.043)
TS14	30	18	7.977	0.394 (±0.065)	0.069 (±0.026)	0.296 (±0.058)	-939.928 (±1633.944	0.069(±0.026)
TS15	13	8	4.471	0.664 (±0.11)	0.76 (±0.098)	0.542 (±0.098)	-539.722 (±761.55	0.76(±0.098)
TS16	14	12	6.059	0.489 (±0.102)	0.308 (±0.117)	0.345 (±0.064)	-659.783 (±798.208	0.308(±0.117)
TS17	20	10	4.166	0.701 (±0.069)	0.411 (±0.107)	0.743 (±0.059)	-559.832 (±760.232	0.411(±0.107)
TS18	14	10	3.818	0.638 (±0.109)	0.622 (±0.088)	0.589 (±0.085)	-459.783 (±705.946	0.622(±0.088)
TS19	19	15	5.014	0.497 (±0.102)	0.177 (±0.046)	0.325 (±0.04)	-859.87 (±728.716	0.177(±0.046)
TS20	10	8	4.424	0.629 (±0.13)	0.876 (±0.117)	0.401 (±0.026)	-579.642 (±758.341	0.876(±0.117)
TS21	14	12	6.484	0.588 (±0.097)	0.413 (±0.088)	0.491 (±0.063)	-399.778 (±728.417	0.413(±0.088)
TS22	11	6	3.409	0.758 (±0.137)	0.943 (±0.044)	0.75 (±0.1)	-459.653 (±645.54	0.943(±0.044)
TS23	34	18	5.437	0.354 (±0.072)	0.039 (±0.025)	0.268 (±0.05)	-519.914 (±886.185	0.039(±0.025)
TS24	18	12	6.127	0.611 (±0.095)	0.29 (±0.091)	0.566 (±0.074)	-579.855 (±702.453	0.29(±0.091)
TS25	22	18	6.385	0.413 (±0.067)	0.155 (±0.024)	0.244 (±0.038)	-759.885 (±938.088	0.155(±0.024)
TS26	14	10	4.786	0.543 (±0.129)	0.477 (±0.161)	0.371 (±0.087)	-439.772 (±643.968	0.477(±0.161)
TS27	18	10	4.726	0.656 (±0.106)	0.435 (±0.14)	0.693 (±0.093)	-639.827 (±749.428	0.435(±0.14)
TS28	15	10	5.168	0.674 (±0.092)	0.56 (±0.105)	0.468 (±0.095)	-559.805 (±732.897	0.56(±0.105)
TS29	48	24	9	0.161 (±0.038)	0.021 (±0.019)	0.201 (±0.029)	-1999.956 (±5038.622	0.021(±0.019)
TS30	22	12	4.907	0.613 (±0.068)	0.21 (±0.065)	0.476 (±0.061)	-599.88 (±728.43	0.21(±0.065)
TS31	60	30	7.129	0.09 (±0.024)	0.024 (±0.011)	0.108 (±0.018)	-4059.964 (±9049.547	0.024(±0.011)
TS32	14	8	4.757	0.716 (±0.093)	0.749 (±0.125)	0.677 (±0.085)	-919.749 (±853.298	0.749(±0.125)
TS33	15	12	6.025	0.578 (±0.1)	0.305 (±0.095)	0.321 (±0.033)	-699.804 (±762.628	0.305(±0.095)
TS34	12	12	7.714	0.551 (±0.089)	0.458 (±0.054)	0.417 (±0)	-519.813 (±677.305	0.458(±0.054)
TS35	15	10	4.709	0.556 (±0.121)	0.526 (±0.115)	0.529 (±0.077)	-539.802 (±787.905	0.526(±0.115)
TS36	12	10	4.811	0.575 (±0.093)	0.653 (±0.131)	0.356 (±0.066)	-559.726 (±732.883	0.653(±0.131)
TS37	7	6	3.755	0.508 (±0.137)	0.945 (±0.058)	0.301 (±0.044)	-899.522 (±677.62	0.945(±0.058)
TS38	36	24	6.097	0.233 (±0.046)	0.057 (±0.02)	0.201 (±0.027)	-1979.941 (±4363.536	0.057(±0.02)
TS39	24	18	5.948	0.381 (±0.08)	0.038 (±0.03)	0.224 (±0.043)	-659.895 (±772.229	0.038(±0.03)
TS40	10	10	5.128	0.216 (±0.168)	0.517 (±0.186)	0.103 (±0.009)	-459.69 (±676.381	0.517(±0.186)
TS41	14	10	4.846	0.54 (±0.124)	0.458 (±0.141)	0.39 (±0.045)	-579.756 (±810.355	0.458(±0.141)
TS42	36	18	7.33	0.381 (±0.052)	0.067 (±0.031)	0.308 (±0.052)	-679.931 (±1719.52	0.067(±0.031)
TS43	38	20	7.817	0.275 (±0.048)	0.043 (±0.015)	0.194 (±0.046)	-1699.94 (±2426.462	0.043(±0.015)
TS44	41	24	9.399	0.19 (±0.049)	0.035 (±0.018)	0.17 (±0.024)	-1739.949 (±4236.91	0.035(±0.018)
TS45	25	20	8.176	0.22 (±0.077)	0.057 (±0.024)	0.166 (±0.03)	-939.905 (±1683.167	0.057(±0.024)
TS46	22	15	7.073	0.462 (±0.082)	0.06 (±0.042)	0.282 (±0.057)	-719.885 (±881.545	0.06(±0.042)
TS47	37	24	6.708	0.188 (±0.053)	0.014 (±0.016)	0.126 (±0.03)	-1499.943 (±2764.575	0.014(±0.016)
TS48	11	6	3.456	0.705 (±0.105)	0.908 (±0.047)	0.875 (±0.075)	-739.692 (±723.081	0.908(±0.047)
TS49	25	24	6.528	0.235 (±0.071)	0.121 (±0.017)	0.122 (±0.006)	-819.916 (±1599.625	0.121(±0.017)
TS50	20	10	4.931	0.718 (±0.08)	0.341 (±0.127)	0.663 (±0.052)	-399.842 (±638.887	0.341(±0.127)

step. We obtained the MATLAB code of PSO from its authors and converted it into C++. The C++ code yields the same solution quality as the MATLAB code but has an additional advantage that we can use it for comparing the execution time. In the TS heuristic, we generated up to 1000 random neighboring solutions of the current solution and selected the best from among them. We defined neighbor solutions as those that differ from each other by only one element. The new solution will replace the current solution if it is better than the current solution (which is the aspiration criterion) or if it does not exist in the Tabu list. The size of the Tabu list was considered equal to 10. In all test cases, the number of trials per problem was equal to fifty.

The tables in the Appendix also contain the results of the heuristics mentioned above. We used the Wilcoxon rank sum test (with a significance level equal to 0.05) to compare the proposed heuristic with the existing ones [35]. Table 4 shows the number of test cases in which the results of the proposed heuristic are significantly better than, equal to, or inferior to the existing heuristics according to the Wilcoxon rank sum test. In the table, the first column provides the maximum allowed runtime and the remaining columns provide the number of test cases in which the proposed heuristic returns a solution which is better, equal or inferior to the heuristic indicated in the heading of the column. The first row of data in the table shows that the when the maximum

TABLE 8. Solution quality of the solutions when the heuristics executed for up to 70 ms.

Problem	N	L	u_{min}	Proposed	Std-SA	IG	PSO	TS
TS1	19	18	8.393	0.104 (±0.085)	0.006 (±0.015)	0.06 (±0.031)	-319.882 (±586.92	0.006(±0.015)
TS2	31	30	9.346	0.028 (±0.025)	0.002 (±0.006)	0.015 (±0.015)	-1579.94 (±2330.719	0.002(±0.006)
TS3	24	20	8.418	0.308 (±0.076)	0.023 (±0.02)	0.11 (±0.035)	-939.905 (±1788.966	0.023(±0.02)
TS4	39	20	8.766	0.327 (±0.044)	0.065 (±0.024)	0.255 (±0.048)	-1159.946 (±2765.381	0.065(±0.024)
TS5	11	10	6.565	0.158 (±0.09)	0.291 (±0.198)	0.091 (±0)	-339.741 (±592.773	0.291(±0.198)
TS6	10	8	4.392	0.687 (±0.108)	0.862 (±0.09)	0.57 (±0.058)	-679.66 (±793.844	0.862(±0.09)
TS7	11	6	3.47	0.811 (±0.112)	0.917 (±0.045)	0.807 (±0.098)	-599.655 (±638.891	0.917(±0.045)
TS8	13	12	5.884	0.45 (±0.141)	0.434 (±0.129)	0.266 (±0.032)	-439.792 (±704.489	0.434(±0.129)
TS9	11	8	3.781	0.577 (±0.152)	0.754 (±0.101)	0.685 (±0.103)	-539.703 (±787.879	0.754(±0.101)
TS10	8	6	3.012	0.636 (±0.083)	0.812 (±0.055)	0.587 (±0.057)	-499.621 (±580.27	0.812(±0.055)
TS11	12	12	7.801	0.093 (±0.057)	0.189 (±0.123)	0.083 (±0)	-359.776 (±692.783	0.189(±0.123)
TS12	48	24	6.448	0.203 (±0.039)	0.029 (±0.019)	0.244 (±0.038)	-1519.945 (±3477.28	0.029(±0.019)
TS13	26	15	5.541	0.485 (±0.081)	0.064 (±0.035)	0.451 (±0.06)	-439.892 (±674.915	0.064(±0.035)
TS14	30	18	7.977	0.438 (±0.068)	0.073 (±0.03)	0.327 (±0.052)	-579.921 (±949.537	0.073(±0.03)
TS15	13	8	4.471	0.701 (±0.115)	0.825 (±0.1)	0.542 (±0.084)	-419.742 (±672.766	0.825(±0.1)
TS16	14	12	6.059	0.504 (±0.111)	0.361 (±0.132)	0.366 (±0.066)	-499.782 (±735.392	0.361(±0.132)
TS17	20	10	4.166	0.716 (±0.059)	0.459 (±0.094)	0.771 (±0.044)	-599.827 (±782.46	0.459(±0.094)
TS18	14	10	3.818	0.69 (±0.128)	0.681 (±0.083)	0.575 (±0.076)	-479.774 (±735.122	0.681(±0.083)
TS19	19	15	5.014	0.512 (±0.088)	0.183 (±0.049)	0.332 (±0.044)	-539.854 (±734.289	0.183(±0.049)
TS20	10	8	4.424	0.63 (±0.104)	0.907 (±0.052)	0.399 (±0.051)	-419.666 (±672.788	0.907(±0.052)
TS21	14	12	6.484	0.6 (±0.099)	0.406 (±0.088)	0.505 (±0.067)	-419.776 (±672.789	0.406(±0.088)
TS22	11	6	3.409	0.793 (±0.128)	0.945 (±0.041)	0.763 (±0.085)	-439.654 (±643.957	0.945(±0.041)
TS23	34	18	5.437	0.374 (±0.061)	0.05 (±0.029)	0.296 (±0.057)	-799.914 (±1261.689	0.05(±0.029)
TS24	18	12	6.127	0.593 (±0.089)	0.329 (±0.101)	0.583 (±0.071)	-479.848 (±762.361	0.329(±0.101)
TS25	22	18	6.385	0.45 (±0.076)	0.16 (±0.024)	0.252 (±0.032)	-459.887 (±613.124	0.16(±0.024)
TS26	14	10	4.786	0.579 (±0.134)	0.568 (±0.152)	0.367 (±0.087)	-539.773 (±761.573	0.568(±0.152)
TS27	18	10	4.726	0.71 (±0.109)	0.569 (±0.105)	0.704 (±0.057)	-679.823 (±740.653	0.569(±0.105)
TS28	15	10	5.168	0.703 (±0.101)	0.627 (±0.108)	0.493 (±0.084)	-319.794 (±620.737	0.627(±0.108)
TS29	48	24	9	0.179 (±0.037)	0.018 (±0.018)	0.206 (±0.028)	-999.952 (±1628.819	0.018(±0.018)
TS30	22	12	4.907	0.623 (±0.075)	0.234 (±0.095)	0.516 (±0.064)	-379.872 (±602.373	0.234(±0.095)
TS31	60	30	7.129	0.093 (±0.021)	0.024 (±0.011)	0.105 (±0.024)	-2999.963 (±7151.424	0.024(±0.011)
TS32	14	8	4.757	0.702 (±0.089)	0.801 (±0.091)	0.68 (±0.088)	-599.741 (±699.835	0.801(±0.091)
TS33	15	12	6.025	0.557 (±0.088)	0.362 (±0.109)	0.333 (±0.044)	-419.805 (±641.722	0.362(±0.109)
TS34	12	12	7.714	0.55 (±0.088)	0.488 (±0.09)	0.417 (±0.002)	-439.8 (±643.932	0.488(±0.09)
TS35	15	10	4.709	0.565 (±0.111)	0.566 (±0.144)	0.528 (±0.068)	-599.803 (±808.116	0.566(±0.144)
TS36	12	10	4.811	0.625 (±0.094)	0.729 (±0.141)	0.365 (±0.058)	-399.736 (±670.038	0.729(±0.141)
TS37	7	6	3.755	0.523 (±0.141)	0.949 (±0.049)	0.305 (±0.056)	-859.522 (±670.348	0.949(±0.049)
TS38	36	24	6.097	0.258 (±0.048)	0.059 (±0.021)	0.217 (±0.029)	-1679.941 (±2113.518	0.059(±0.021)
TS39	24	18	5.948	0.414 (±0.088)	0.045 (±0.027)	0.237 (±0.033)	-519.89 (±677.334	0.045(±0.027)
TS40	10	10	5.128	0.174 (±0.119)	0.622 (±0.183)	0.103 (±0.009)	-479.693 (±735.071	0.622(±0.183)
TS41	14	10	4.846	0.519 (±0.095)	0.458 (±0.158)	0.392 (±0.046)	-539.766 (±734.256	0.458(±0.158)
TS42	36	18	7.33	0.406 (±0.048)	0.071 (±0.028)	0.329 (±0.061)	-439.929 (±907.118	0.071(±0.028)
TS43	38	20	7.817	0.291 (±0.05)	0.044 (±0.02)	0.221 (±0.054)	-1419.941 (±1604.714	0.044(±0.02)
TS44	41	24	9.399	0.229 (±0.043)	0.033 (±0.016)	0.179 (±0.031)	-2719.947 (±4798.125	0.033(±0.016)
TS45	25	20	8.176	0.263 (±0.074)	0.054 (±0.019)	0.178 (±0.031)	-639.908 (±749.416	0.054(±0.019)
TS46	22	15	7.073	0.5 (±0.07)	0.061 (±0.041)	0.315 (±0.043)	-579.882 (±672.781	0.061(±0.041)
TS47	37	24	6.708	0.205 (±0.043)	0.016 (±0.012)	0.143 (±0.034)	-839.936 (±1345.598	0.016(±0.012)
TS48	11	6	3.456	0.701 (±0.12)	0.922 (±0.049)	0.871 (±0.073)	-739.702 (±694.263	0.922(±0.049)
TS49	25	24	6.528	0.238 (±0.081)	0.123 (±0.019)	0.124 (±0.007)	-339.91 (±658.078	0.123(±0.019)
TS50	20	10	4.931	0.713 (±0.065)	0.452 (±0.12)	0.667 (±0.061)	-459.829 (±705.958	0.452(±0.12)

allowed runtime of the heuristics is 40 ms, then the proposed heuristic is better than IG, PSO, std-SA, and TS in up to 39, 47, 39, and 47 test cases, respectively. The proposed heuristic has solution quality equal to IG, PSO, std-SA, and TS in 5, 3, 2, and 3 test cases, respectively. The solution quality of the proposed heuristic is less than that of IG, std-SA and TS in 6, 0, 9, and 0 test cases, respectively. The remaining rows show the results of the comparison when the maximum runtime of the heuristics in 50 ms, 60 ms, 70 ms, and 80 ms. The results show that the proposed heuristic outperforms the existing heuristics with respect to solution quality.

In Figs. 12 and 13, we show the percentage deviation between the mean values of the proposed heuristic and the existing heuristics. The positive values indicate that the mean of the proposed heuristic is better than the existing one. The y-axis in Figs. 12 is upper bounded to 300% deviation. As the graphs shows, at both execution timings (40 or 80 ms), the mean of proposed heuristic is significantly better than that of the existing ones.

V. CONCLUSION

In this paper, we considered a multi-user DC-OFDM based VLC system and investigated how to optimally determine the allocation of the users to different LEDs and subcarriers. We formulated the resource allocation problem as the maximization of user satisfaction index and presented a SA based

TABLE 9. Solution quality of the solutions when the heuristics executed for up to 80 ms.

Problem	N	L	u_{min}	Proposed	Std-SA	IG	PSO	TS
TS1	19	18	8.393	0.097 (±0.076)	0.013 (±0.024)	0.06 (±0.027)	-219.885 (±464.647	0.013(±0.024)
TS2	31	30	9.346	0.034 (±0.028)	0.004 (±0.008)	0.014 (±0.015)	-999.937 (±2498.977	0.004(±0.008)
TS3	24	20	8.418	0.313 (±0.076)	0.029 (±0.023)	0.124 (±0.023)	-679.895 (±740.654	0.029(±0.023)
TS4	39	20	8.766	0.372 (±0.046)	0.069 (±0.023)	0.289 (±0.041)	-1099.942 (±2140.472	0.069(±0.023)
TS5	11	10	6.565	0.22 (±0.117)	0.353 (±0.186)	0.091 (±0)	-459.714 (±645.504	0.353(±0.186)
TS6	10	8	4.392	0.646 (±0.1)	0.913 (±0.05)	0.569 (±0.053)	-539.668 (±734.286	0.913(±0.05)
TS7	11	6	3.47	0.774 (±0.109)	0.914 (±0.046)	0.81 (±0.113)	-539.649 (±613.141	0.914(±0.046)
TS8	13	12	5.884	0.473 (±0.131)	0.549 (±0.137)	0.267 (±0.024)	-739.773 (±852.593	0.549(±0.137)
TS9	11	8	3.781	0.609 (±0.16)	0.809 (±0.086)	0.673 (±0.138)	-459.698 (±734.252	0.809(±0.086)
TS10	8	6	3.012	0.635 (±0.09)	0.824 (±0.047)	0.598 (±0.058)	-519.615 (±646.492	0.824(±0.047)
TS11	12	12	7.801	0.083 (±0)	0.205 (±0.126)	0.087 (±0.024)	-439.791 (±732.875	0.205(±0.126)
TS12	48	24	6.448	0.211 (±0.044)	0.032 (±0.015)	0.253 (±0.033)	-939.944 (±2393.964	0.032(±0.015)
TS13	26	15	5.541	0.497 (±0.089)	0.087 (±0.044)	0.471 (±0.06)	-599.895 (±755.932	0.087(±0.044)
TS14	30	18	7.977	0.452 (±0.062)	0.074 (±0.03)	0.353 (±0.055)	-519.915 (±862.838	0.074(±0.03)
TS15	13	8	4.471	0.673 (±0.107)	0.847 (±0.085)	0.537 (±0.091)	-399.724 (±638.854	0.847(±0.085)
TS16	14	12	6.059	0.474 (±0.108)	0.419 (±0.158)	0.392 (±0.07)	-639.78 (±851.399	0.419(±0.158)
TS17	20	10	4.166	0.735 (±0.063)	0.573 (±0.12)	0.783 (±0.042)	-399.832 (±638.877	0.573(±0.12)
TS18	14	10	3.818	0.685 (±0.114)	0.739 (±0.095)	0.621 (±0.084)	-539.762 (±761.577	0.739(±0.095)
TS19	19	15	5.014	0.533 (±0.098)	0.215 (±0.072)	0.356 (±0.043)	-539.864 (±761.576	0.215(±0.072)
TS20	10	8	4.424	0.647 (±0.096)	0.906 (±0.054)	0.406 (±0.029)	-379.62 (±696.644	0.906(±0.054)
TS21	14	12	6.484	0.597 (±0.09)	0.466 (±0.114)	0.491 (±0.065)	-519.776 (±788.681	0.466(±0.114)
TS22	11	6	3.409	0.774 (±0.126)	0.933 (±0.04)	0.78 (±0.102)	-439.648 (±611.471	0.933(±0.04)
TS23	34	18	5.437	0.4 (±0.055)	0.04 (±0.024)	0.333 (±0.056)	-579.915 (±859.294	0.04(±0.024)
TS24	18	12	6.127	0.632 (±0.113)	0.386 (±0.105)	0.568 (±0.056)	-439.843 (±704.491	0.386(±0.105)
TS25	22	18	6.385	0.446 (±0.08)	0.16 (±0.029)	0.266 (±0.034)	-559.88 (±732.901	0.16(±0.029)
TS26	14	10	4.786	0.571 (±0.142)	0.686 (±0.124)	0.371 (±0.075)	-459.751 (±761.562	0.686(±0.124)
TS27	18	10	4.726	0.733 (±0.113)	0.647 (±0.128)	0.718 (±0.068)	-839.825 (±765.589	0.647(±0.128)
TS28	15	10	5.168	0.694 (±0.103)	0.719 (±0.094)	0.528 (±0.09)	-359.792 (±721.681	0.719(±0.094)
TS29	48	24	9	0.196 (±0.047)	0.018 (±0.015)	0.213 (±0.026)	-1139.947 (±2240.722	0.018(±0.015)
TS30	22	12	4.907	0.633 (±0.1)	0.282 (±0.087)	0.522 (±0.076)	-519.86 (±735.132	0.282(±0.087)
TS31	60	30	7.129	0.112 (±0.027)	0.025 (±0.012)	0.112 (±0.022)	-5059.962 (±9813.382	0.025(±0.012)
TS32	14	8	4.757	0.703 (±0.108)	0.871 (±0.092)	0.714 (±0.082)	-579.735 (±810.378	0.871(±0.092)
TS33	15	12	6.025	0.552 (±0.095)	0.388 (±0.121)	0.344 (±0.037)	-759.789 (±822.114	0.388(±0.121)
TS34	12	12	7.714	0.582 (±0.092)	0.49 (±0.073)	0.417 (±0)	-439.808 (±704.466	0.49(±0.073)
TS35	15	10	4.709	0.564 (±0.124)	0.679 (±0.141)	0.549 (±0.088)	-639.793 (±802.044	0.679(±0.141)
TS36	12	10	4.811	0.601 (±0.084)	0.843 (±0.099)	0.361 (±0.066)	-659.725 (±717.426	0.843(±0.099)
TS37	7	6	3.755	0.526 (±0.165)	0.946 (±0.047)	0.294 (±0.05)	-719.522 (±640.147	0.946(±0.047)
TS38	36	24	6.097	0.283 (±0.043)	0.063 (±0.019)	0.223 (±0.034)	-979.937 (±1597.07	0.063(±0.019)
TS39	24	18	5.948	0.412 (±0.07)	0.059 (±0.043)	0.235 (±0.042)	-499.89 (±614.462	0.059(±0.043)
TS40	10	10	5.128	0.218 (±0.176)	0.7 (±0.148)	0.102 (±0.008)	-459.688 (±734.247	0.7(±0.148)
TS41	14	10	4.846	0.529 (±0.104)	0.589 (±0.112)	0.408 (±0.046)	-439.737 (±732.868	0.589(±0.112)
TS42	36	18	7.33	0.454 (±0.063)	0.073 (±0.032)	0.357 (±0.062)	-519.927 (±931.095	0.073(±0.032)
TS43	38	20	7.817	0.316 (±0.049)	0.053 (±0.018)	0.24 (±0.054)	-959.933 (±1211.503	0.053(±0.018)
TS44	41	24	9.399	0.258 (±0.06)	0.039 (±0.02)	0.192 (±0.029)	-1059.947 (±1570.261	0.039(±0.02)
TS45	25	20	8.176	0.29 (±0.084)	0.066 (±0.03)	0.182 (±0.029)	-639.902 (±851.402	0.066(±0.03)
TS46	22	15	7.073	0.502 (±0.088)	0.071 (±0.046)	0.307 (±0.05)	-539.881 (±676.417	0.071(±0.046)
TS47	37	24	6.708	0.247 (±0.057)	0.016 (±0.017)	0.154 (±0.03)	-1919.942 (±4178.865	0.016(±0.017)
TS48	11	6	3.456	0.771 (±0.119)	0.926 (±0.042)	0.894 (±0.053)	-779.686 (±678.815	0.926(±0.042)
TS49	25	24	6.528	0.263 (±0.09)	0.124 (±0.015)	0.124 (±0.007)	-539.905 (±885.497	0.124(±0.015)
TS50	20	10	4.931	0.726 (±0.071)	0.556 (±0.116)	0.699 (±0.049)	-639.832 (±776.172	0.556(±0.116)

iterative heuristic solution. In an effort to keep the runtime less than the coherence time of the VLC channel, we utilized a new representation using a BG and proposed a neighbor function that works with this representation. The representation ensures that moves will take the search to valid states, and the algorithm can provide good solutions in acceptable time. We ran our heuristic on a diverse set of test cases with different number of users and LEDs. The simulation results showed that the proposed heuristic can produce good quality solutions using a minimal runtime (40 to 80 ms). For example, when the maximum runtime is 60ms, the average required-data-rate of users is 10 Mbps, and the number of users and LEDs lies between 11-20 and 6-10, respectively; the proposed heuristic

on can achieve average user satisfaction indices between 72-77%. We also compared our heuristic with standard SA and two existing heuristics and found that the proposed heuristic is significantly better than the existing ones.

APPENDIX

This appendix presents the detailed simulation results. Tables 5, 6, 7, 8. and 9 show the results of the experiments when the maximum allowed execution time of the heuristics is 40 ms, 50 ms, 60 ms, 70 ms, and 80 ms, respectively. In the tables, the first column indicates the problem name, the second, third and fourth columns show the number of users, number of LEDs, and the minimum distance between

any two users, respectively. The fifth, sixth, seventh, and eighth columns contain the solution quality (average of the user satisfaction indices of all users) of the proposed heuristic, std-SA, IG, and PSO, respectively. We have expressed the solution quality in the format as ''average value $\pm$ (standard deviation)''.

REFERENCES

[1] S. Arnon, J. Barry, G. Karagiannidis, R. Schober, and M. Uysal, *Advanced Optical Wireless Communication Systems*. Cambridge, U.K.: Cambridge Univ. Press, 2012.

[2] J. Armstrong, ''OFDM for optical communications,'' *J. Lightw. Technol.*, vol. 27, no. 3, pp. 189–204, Feb. 1, 2009.

[3] J. Armstrong and A. J. Lowery, ''Power efficient optical OFDM,'' *Electron. Lett.*, vol. 42, no. 6, pp. 370–372, Mar. 2006.

[4] D. Tsonev, S. Sinanovic, and H. Haas, ''Novel unipolar orthogonal frequency division multiplexing (U-OFDM) for optical wireless,'' in *Proc. IEEE 75th Veh. Technol. Conf. (VTC)*, May 2012, pp. 1–5.

[5] N. Fernando, Y. Hong, and E. Viterbo, ''Flip-OFDM for unipolar communication systems,'' *IEEE Trans. Commun.*, vol. 60, no. 12, pp. 3726–3733, Dec. 2012.

[6] D. Tsonev, S. Videv, and H. Haas, ''Unlocking spectral efficiency in intensity modulation and direct detection systems,'' *IEEE J. Sel. Areas Commun.*, vol. 33, no. 9, pp. 1758–1770, Sep. 2015.

[7] M. Ulema *et al.*, ''Standards news,'' *IEEE Commun. Standards Mag.*, vol. 1, no. 3, pp. 13–19, Sep. 2017.

[8] Y. Wang, X. Wu, and H. Haas, ''Resource allocation in LiFi OFDMA systems,'' in *Proc. IEEE Global Commun. Conf. (GLOBECOM)*, Dec. 2017, pp. 1–6.

[9] D. Bykhovsky and S. Arnon, ''Multiple access resource allocation in visible light communication systems,'' *J. Lightw. Technol.*, vol. 32, no. 8, pp. 1594–1600, Apr. 15, 2014.

[10] X. Ling, J. Wang, Z. Ding, C. Zhao, and X. Gao, ''Efficient OFDMA for LiFi downlink,'' *J. Lightw. Technol.*, vol. 36, no. 10, pp. 1928–1943, May 15, 2018.

[11] F. Seguel, I. Soto, D. Iturralde, P. Adasme, and B. Nuñez, ''Enhancement of the QoS in an OFDMA/VLC system,'' in *Proc. 10th Int. Symp. Commun. Syst., Netw. Digit. Signal Process. (CSNDSP)*, Jul. 2016, pp. 1–5.

[12] D. Rodrigues *et al.*, ''BCS: A binary cuckoo search algorithm for feature selection,'' in *Proc. IEEE Int. Symp. Circuits Syst. (ISCAS)*, May 2013, pp. 465–468.

[13] S. M. Sait and H. Youssef, *Iterative Computer Algorithms With Applications in Engineering: Solving Combinatorial Optimization Problems*, 1st ed. Los Alamitos, CA, USA: IEEE Computer Society Press, 1999.

[14] S. Feng, R. Zhang, X. Li, Q. Wang, and L. Hanzo, ''Dynamic throughput maximization for the user-centric visible light downlink in the face of practical considerations,'' *IEEE Trans. Wireless Commun.*, vol. 17, no. 8, pp. 5001–5015, Aug. 2018.

[15] M. S. Demir, O. F. Gemici, and M. Uysal, ''Genetic algortihm based resource allocation technique for VLC networks,'' in *Proc. 25th Signal Process. Commun. Appl. Conf. (SIU)*, May 2017, pp. 1–4.

[16] M. S. Demir, S. M. Sait, and M. Uysal, ''Unified resource allocation and mobility management technique using particle swarm optimization for VLC networks,'' *IEEE Photon. J.*, vol. 10, no. 6, Dec. 2018, Art. no. 7908809.

[17] M. D. Soltani, A. A. Purwita, Z. Zeng, H. Haas, and M. Safari, ''Modeling the random orientation of mobile devices: Measurement, analysis and LiFi use case,'' *IEEE Trans. Commun.*, vol. 67, no. 3, pp. 2157–2172, Mar. 2019.

[18] R. C. Kizilirmak, O. Narmanlioglu, and M. Uysal, ''Centralized light access network (C-LiAN): A novel paradigm for next generation indoor VLC networks,'' *IEEE Access*, vol. 5, pp. 19703–19710, 2017.

[19] Y. Wang, X. Wu, and H. Haas, ''Load balancing game with shadowing effect for indoor hybrid LiFi/RF networks,'' *IEEE Trans. Wireless Commun.*, vol. 16, no. 4, pp. 2366–2378, Apr. 2017.

[20] K. Seo, S. Hyun, and Y.-H. Kim, ''An edge-set representation based on a spanning tree for searching cut space,'' *IEEE Trans. Evol. Comput.*, vol. 19, no. 4, pp. 465–473, Aug. 2015.

[21] J. Honda and H. Yamamoto, ''Variable length lossy coding using an LDPC code,'' *IEEE Trans. Inf. Theory*, vol. 60, no. 1, pp. 762–775, Jan. 2014.

[22] A. Adler, M. Elad, and Y. Hel-Or, ''Linear-time subspace clustering via bipartite graph modeling,'' *IEEE Trans. Neural Netw. Learn. Syst.*, vol. 26, no. 10, pp. 2234–2246, Oct. 2015.

[23] S. M. Sait and H. Youssef, *VLSI Physical Design Automation: Theory and Practice*. Singapore: World Scientific, 1999.

[24] I. Stefan and H. Haas, ''Analysis of optimal placement of led arrays for visible light communication,'' in *Proc. IEEE 77th Veh. Technol. Conf. (VTC Spring)*, Jun. 2013, pp. 1–5.

[25] U. F. Siddiqi and S. M. Sait. *Test Problems*. Accessed: Feb. 11, 2019. [Online]. Available: https://sites.google.com/view/vlctestproblems

[26] (2018). *Soleriq S 9, GW KAFHB5.EM Datasheet*. [Online]. Available: https://dammedia.osram.info/media/resource/hires/osram-dam-5141332/GW%20KAFHB5.EM_EN.pdf

[27] S. Dimitrov and H. Haas, ''Information rate of OFDM-based optical wireless communication systems with nonlinear distortion,'' *J. Lightw. Technol.*, vol. 31, no. 6, pp. 918–929, Mar. 15, 2013.

[28] D. Tsonev, S. Sinanovic, and H. Haas, ''Complete modeling of nonlinear distortion in OFDM-based optical wireless communication,'' *J. Lightw. Technol.*, vol. 31, no. 18, pp. 3064–3076, Sep. 15, 2013.

[29] P. Aggarwal, R. Ahmad, V. A. Bohara, and A. Srivastava, ''Adaptive predistortion technique for nonlinear LED with dimming control in VLC system,'' in *Proc. IEEE Int. Conf. Adv. Netw. Telecommun. Syst. (ANTS)*, Dec. 2017, pp. 1–6.

[30] H. Elgala, R. Mesleh, and H. Haas, ''Predistortion in optical wireless transmission using OFDM,'' in *Proc. 9th Int. Conf. Hybrid Intell. Syst. (HIS)*, vol. 2, Aug. 2009, pp. 184–189.

[31] M. Zhang and Z. Zhang, ''An optimum DC-biasing for DCO-OFDM system,'' *IEEE Commun. Lett.*, vol. 18, no. 8, pp. 1351–1354, Aug. 2014.

[32] C. Chen, M. Ijaz, D. Tsonev, and H. Haas, ''Analysis of downlink transmission in DCO-OFDM-based optical attocell networks,'' in *Proc. IEEE Global Commun. Conf.*, Dec. 2014, pp. 2072–2077.

[33] T. Komine and M. Nakagawa, ''Fundamental analysis for visible-light communication system using LED lights,'' *IEEE Trans. Consum. Electron.*, vol. 50, no. 1, pp. 100–107, Feb. 2004.

[34] T. Stützle and R. Ruiz, ''Iterated greedy,'' in *Handbook of Heuristics*. Cham, Switzerland: Springer, 2017, pp. 1–31. doi: 10.1007/978-3-319-07153-4_10-1.

[35] U. F. Siddiqi and S. M. Sait, ''An optimization heuristic based on nondominated sorting and tabu search for the fixed spectrum frequency assignment problem,'' *IEEE Access*, vol. 6, pp. 72635–72648, 2018.

UMAIR F. SIDDIQI (M'12) was born in Karachi, Pakistan, in 1979. He received the B.E. degree in electrical engineering from the NED University of Engineering and Technology, Karachi, in 2002, the M.Sc. degree in computer engineering from the King Fahd University of Petroleum & Minerals (KFUPM), Dhahran, Saudi Arabia, in 2007, and the Dr.Eng. degree from Gunma University, Japan, in 2013. He is currently a Research Engineer with the Center of Communications and Information Technology Research, Research Institute, KFUPM. He has authored over 30 research papers in international journals and conferences. He holds two U.S. patents. His research interests include optimization, metaheuristics, soft computing, and deep learning.

SADIQ M. SAIT was born in Bengaluru, India. He received the bachelor's degree in electronics engineering from Bangalore University, in 1981, and the master's and Ph.D. degrees in electrical engineering from KFUPM, in 1983 and 1987, respectively. He is currently a Professor of computer engineering and the Director of the Center for Communications and IT Research, KFUPM. He has authored over 200 research papers, contributed chapters to technical books, and lectured in over 25 countries. He is also the principle author of two books. In 1981, he received the Best Electronic Engineer Award from the Indian Institute of Electrical Engineers, Bengaluru.

M. SELIM DEMIR was born in Aksaray, Turkey, in 1984. He received the B.S. degree in telecommunication engineering from Istanbul Technical University, Istanbul, Turkey, in 2007, and the M.S. degree in electrical engineering from Columbia University, New York, NY, USA, in 2010. He is currently pursuing the Ph.D. degree in electrical and electronics engineering with Özyeğin University, Istanbul. Since 2011, he has been a Researcher with TUBITAK BILGEM. His research interests include the visible light communication and communication networks.

MURAT UYSAL received the B.Sc. and M.Sc. degrees in electronics and communication engineering from Istanbul Technical University, Istanbul, Turkey, in 1995 and 1998, respectively, and the Ph.D. degree in electrical engineering from Texas A&M University, College Station, TX, USA, in 2001. He is currently a Full Professor and the Chair of the Department of Electrical and Electronics Engineering, Özyeğin University, Istanbul. He also serves as the Founding Director of the Center of Excellence in Optical Wireless Communication Technologies. Prior to joining Özyeğin University, he was a tenured Associate Professor with the University of Waterloo, Canada, where he still holds an Adjunct Faculty position. His research interests include the broad areas of communication theory and signal processing, with a particular emphasis on the physical-layer aspects of wireless communication systems in radio and optical frequency bands. He has authored some 290 journals and conference papers in his research topics and received more than 7500 citations. His distinctions include the Marsland Faculty Fellowship, in 2004, the NSERC Discovery Accelerator Supplement Award, in 2008, the University of Waterloo Engineering Research Excellence Award, in 2010, the Turkish Academy of Sciences Distinguished Young Scientist Award, in 2011, and the Özyeğin University Best Researcher Award, in 2014. He has served as the Chair of the Communication Theory Symposium of the IEEE ICC 2007, the Communications and Networking Symposium of the IEEE CCECE 2008, and the Communication and Information Theory Symposium of the IWCMC 2011, the TPC Co-Chair of the IEEE WCNC 2014, and the General Chair of the IEEE IWOW 2015. He currently serves on the Editorial Board of the IEEE Transactions on Wireless Communications. He was involved in the organization of several IEEE conferences at various levels. Over the years, he has served on the technical program committees of more than 100 international conferences and workshops in the communications area. In the past, he was an Editor of the IEEE Transactions on Communications, the IEEE Transactions on Vehicular Technology, the IEEE Communications Letters, *Wireless Communications and Mobile Computing* journal, and *Transactions on Emerging Telecommunications Technologies*. He was the Guest Editor of the IEEE Journal on Selected Areas in Communications Special Issues on Optical Wireless Communication, in 2009 and 2015.

. . .